

Stabilizing single atom contacts by molecular bridge formation

November 6, 2018

Everardus H. Huisman^{*†}, Marius L. Trouwborst[†], Frank L. Bakker[†], Bert de Boer[†], Bart J. van Wees[†], Sense J. van der Molen[‡]

*Zernike Institute for Advanced Materials, University of Groningen, Nijenborgh 4, 9747 AG Groningen, The Netherlands, and Kamerlingh Onnes Laboratory, Leiden University, Niels Bohrweg 2, 2333 CA Leiden, The Netherlands*¹

Abstract

Gold-molecule-gold junctions can be formed by carefully breaking a gold wire in a solution containing dithiolated molecules. Surprisingly, there is little understanding on the mechanical details of the bridge formation process and specifically on the role that the dithiol molecules play themselves. We propose that alkanedithiol molecules have already formed bridges between the gold electrodes *before* the atomic gold-gold junction is broken. This leads to stabilization of the single atomic gold junction, as observed experimentally. Our data can be understood within a simple spring model.

A single molecule forms a potential electronic component, offering the perspective of true bottom up engineering of nanodevices. Functionalities such as switching [1] [2] and rectifying [3] have been demonstrated in the past years. Nevertheless, the field of molecular electronics has been troubled by difficulties in making reliable and well-defined contacts to single molecules. Fortunately, recent times have seen a significant growth of independent techniques to contact single molecules or small ensembles of molecules [4] [5]. An important contribution to this development was made by Xu and Tao, who used a scanning tunneling microscope (STM) to contact dithiolated

¹†University of Groningen ‡University of Leiden and University of Groningen, *Corresponding author email address: e.h.huisman@rug.nl

molecules [6]. In these experiments, a gold STM-tip is carefully pulled out of contact with a gold substrate in the presence of a solution. Simultaneously, the conductance G of the tip-substrate junction is measured. As the tip is pulled up, the diameter of the gold neck connecting tip and substrate becomes smaller and hence G decreases. This process is continued down to the limit of a single gold atom contact, in which case G reaches a value around $1G_0 = 2e^2/h = 77.5\mu S$, the quantum of conductance. Pulling further, one observes a sudden downward jump in the conductance, indicative of the breaking of the gold constriction. This 'jump out of contact' (JOC) has been thoroughly studied by several groups [7, 8]. Xu and Tao made the remarkable observation that a gold-molecule-gold contact may form after JOC, provided molecules with suitable anchor groups (such as thiol groups) are present in the solution [6]. The molecular junctions thus created have a limited life time and a conductance that varies from experiment to experiment. Therefore, it is pivotal to carefully study the statistics of many of such 'break junction' traces. Several groups have adopted the Tao method since, either using scanning tunneling microscopy break junctions (STM-BJ) [9, 10, 11, 12], or mechanically controllable break junctions (MCBJ) [13]. Although the procedure is applied to a variety of molecules [14, 15, 16], many studies have focused on simple alkanedithiol molecules in order to create a well-defined reference point for molecular electronics [9, 10, 11, 12, 13, 17, 18, 19]. Despite these efforts, remarkably little is known about the mechanism of molecular bridge formation. Here, we will address this important, but relatively untouched issue.

On our quest, we focus on the moment right before the jump out of contact. At that instance, the dithiol molecule(s) that will later form the bridge are either connected to one (scenario I in Figure 1(a)) or to both electrodes (scenario II). A situation in which no dithiol molecules are connected to the gold contacts prior to breaking is highly unlikely due to the strong tendency of Au-S bond formation. Interestingly, both scenario I and II can evolve into a metal-molecule-metal bridge. In I, the metal-molecule-metal bridge is formed after JOC, when the loose end of the molecule binds to the other electrode. In II, the molecule already bridges both sides of the electrodes before JOC. The presence of such molecular bridges would not be obvious from the conductance value itself, due to the much higher parallel current flowing through the gold neck. However, the atomic junction would be reinforced by parallel molecular bridges, leading to a higher mechanical stability of the gold constriction. After the atomic junction breaks down, the conductance of a molecular bridge can finally be determined. In this Letter, we provide evidence for scenario II. Our experimental results are discussed in the light of a simple spring model.

For our experiments, we use lithographically defined MCBJs, submerged in a toluene solution [13, 20]. A schematic representation of the set-up is given in Figure 1 (b). In short, a MCBJ consists of a gold wire with a constriction in its center, attached to a flexible substrate (see Figure 1 (b,c)) [7]. The substrate is bent in a 3-point bending mechanism, by moving a pushing rod upwards with a motor. As a result, the central constriction is gently elongated, until it finally breaks. After this, the distance between the two freshly created electrodes, d , is related to pushing rod position, Z , by the attenuation factor, $r = \Delta d / \Delta z = \zeta 6ut / L^2$. Here u is the length of the bridge, L is the distance between the counter supports and t is the thickness of the substrate. For lithographic MCBJs, r should incorporate a factor ζ to correct for the presence of a soft (polyimide) layer [21]. To fabricate such MCBJs, a gold (99.99%, Umicore) wire of 100 nm wide and 120 nm thick (using a 1 nm Cr adhesion layer) is thermally evaporated on top of a pyrralin polyimide coated phosphor bronze substrate ($22.5 \times 10.5 \times 0.5$ mm) with standard lift-off based e-beam lithography. The central constriction is made free hanging by reactive ion etching with an O_2/CF_4 plasma (see Figure 1 (c)). Calibrating the junctions in argon we find, $\zeta = 4.5$ and $r \approx 7.7 \cdot 10^{-5}$ for our specific geometry ($u = 2.7 \mu\text{m}$, $L = 20$ mm, $t = 0.42$ mm). Hence, d can be controlled with sub-Å resolution, with a drift of less than 1 pm/min at room temperature. The conductance of the junction is measured by applying a 100 mV bias, while sampling the current at 5 kHz with a 16-bit National Instruments data acquisition board via a home-built trans impedance amplifier ($1 \mu\text{A/V}$) [13, 20]. We add a series resistance to limit the total current ($101.3 \text{ k}\Omega$) at low junction resistances (thereby decreasing the effective bias felt by the junction). As a solvent, we choose nitrogen-saturated toluene (see Supporting Information) due to its good solubility for organic molecules, low conductivity and low hygroscopy. Alkanedithiol molecules, i.e., 1,4-butanedithiol (BDT) and 1,8-octanedithiol (ODT), were obtained from Sigma-Aldrich.

After mounting the sample and the liquid cell, we flush with 40 ml of toluene. Subsequently, we introduce 20 ml of the solution of interest, which is either pure toluene or toluene with a concentration of 10 mM alkanedithiols. Next, we start breaking and rejoining the gold junction by moving the pushing rod up and down. Traces of conductance versus pushing rod position, $G(Z)$, are recorded with a pushing rod speed of $+15 \mu\text{m/s}$, corresponding to a local elongation of 1.1 nm/s. After having reached the lowest measurable current (just above 10^{-11} A), we push another $30 \mu\text{m}$ in Z in order to allow diffusion of molecules in between the electrodes. Then, the junction is closed again to a conductance value of $\sim 10 G_0$ in order to randomize the atoms and molecules involved.

The inset of Figure 2 displays 3 typical opening traces on a semilog plot in pure toluene, i.e., without dithiols (black). While breaking gold nanowires, we distinguish 2 different regimes: the contact regime and the out-of-contact regime. In the contact regime the conductance is given by the Landauer formula: $G = G_0 \sum T_n$, where T_n is the transmission probability of the n^{th} channel. A single gold atom acts as a waveguide for electrons and forms a single channel [7, 22, 23]. In our experiments this is especially visible just before breaking, when only one atom bridges the electrodes. Due to the stability of this conformation, plateaus at a constant conductance value around $1 G_0$ appear. This plateau abruptly ends by a JOC to lower conductances (the out-of-contact regime) within 1 ms. When the junction breaks for the first time, the conductance after JOC drops to values below $10^{-5} G_0$ (the first black trace in the inset of Figure 2). Usually, within tens of traces the conductance just after JOC increases to values around $1 \cdot 10^{-3} G_0$. At low temperatures, we have previously showed that the size of JOC can be controlled by 'training' the contact [8]. This procedure reduces the number of atoms involved in the breaking, eventually till the ultimate limit of 2 atoms. We have explored the possibility of 'training' electrodes at room temperature, thereby reducing JOC. We found that the high mobility of gold atoms at elevated temperatures make this procedure cumbersome. After JOC, G decays roughly exponentially with d as is expected for tunneling. Using the fact that the tunneling decay constant in toluene is roughly the same as in vacuum ($1 \text{ dec}/\text{\AA}$) [20], we can relate the actual jump in conductance to a electrode distance of about 3 \AA .

In the main panel of Figure 2, a histogram for pure toluene (black, solid line) incorporating all 250 opening traces in 1000 logarithmic bins is shown. Such a representation, allows for a broad overview of the entire data set, while correcting for background tunneling in a natural way [13]. We emphasize that we did not select traces. In the contact regime, the histogram shows peaks at (integer values of) $1 G_0$, as will be discussed in more detail below. In the out-of-contact regime, the histogram is relatively featureless, except for the lack of points in the regime where the jump out of contact takes place ($1G_0 > G > 3 \cdot 10^{-3}G_0$). Most importantly, we note that for $G < 3 \cdot 10^{-3}G_0$, the number of points per bin is roughly constant. This is a result of the exponential decay in G due to tunnelling in pure toluene.

Next, we repeat the experiment in the presence of ODT molecules (10 mM in toluene). In that case, additional plateaus of constant conductance appear in the out-of-contact regime in about 20 % of the opening traces (red traces in the inset of Figure 2). These plateaus are usually shorter than the ones at $1 G_0$ and show fluctuations in the conductance. They are interpreted as the signature of gold-molecule-gold bridges. To obtain a statistically sound

value for the conductance of an ODT molecular bridge, we collect all 250 traces in a logarithmic histogram (red line in the main panel of Figure 2). The conductance plateaus discussed above, result in a peak around $G = 4 \cdot 10^{-5} G_0$, related to molecular bridge formation. The average conductance we find for ODT bridges is in good agreement with the work by González *et al.*, which was done under similar circumstances [13]. Furthermore, it is in correspondence with the so-called 'low peaks' in the work of the Tao group [9] and the 'medium peaks' in the work of the Wandlowski group [10]. When adding a shorter molecule, i.e., BDT, an interesting contrast is found with the case of ODT. For BDT, no additional peaks appear in the out-of-contact regime (green traces and green histogram in Figure 2).

Having discussed the out-of-contact regime, where the conductance values of molecular bridges can be directly distinguished, we focus on another remarkable difference between toluene and dithiol experiments. For this, we concentrate on the contact regime, i.e., before the atomically thin gold neck is broken. The formation of single or few atomic gold junctions during breaking gives rise to plateaus around (multiples of) G_0 (inset Figure 2). In histograms, this translates to peaks (main panel of Figure 2). Interestingly, these peaks are significantly larger in the presence of BDT and ODT than for pure toluene. This effect (both in peak height and area) is especially clear around $1 G_0$. A first, rather trivial possibility would be that the addition of dithiols to toluene may lead to a decrease in the attenuation factor r . A smaller r would give rise to a lower local velocity $\Delta d/\Delta t$ and therefore to more points per bin. This effect should be especially clear in the tunnel regime, which is very sensitive to variations in distance. In a logarithmic representation, a lower r should yield a higher constant background in the out-of-contact regime [13]. However, besides the ODT peak around $4 \cdot 10^{-5} G_0$, no apparent increase in counts is observed in the out-of-contact regime for both ODT and BDT (say for $10^{-4} G_0 < G < 3 \cdot 10^{-3} G_0$). This rules out a variation of r , indicating that the presence of dithiols truly stabilizes atomic contacts. To substantiate this, histograms of the length of the G_0 plateaus were constructed for all experiments (Figure 3). The plateau length is defined as the length (in units of Z) of the plateau between 0.5 and $1.5 G_0$. We summarized the average plateau length of 7 different data sets (3 times pure toluene, 2 times 10 mM BDT and 2 times 10 mM ODT) in Table 1. Clearly, the effect reproduces using different samples and the $1 G_0$ plateau length shifts towards higher values in going from toluene (average value of $0.7 \mu\text{m}$) to ODT and BDT ($1.6 \mu\text{m}$ and $2.0 \mu\text{m}$, respectively). Note that these plateau length values correspond to a displacement close to the diameter of a gold atom ($\frac{0.25\text{nm}}{r} = 3.3\mu\text{m}$), indicating that no chains of atoms are formed during the breaking procedure [24]. We conclude that, in the presence of

dithiols, the electrodes have to be displaced over a larger distance to break the gold-gold junction. In other words, alkanedithiols reinforce the atomic gold junction. This is fully consistent with scenario II (Figure 1(a)), in which molecular bridges have already formed before the gold neck breaks.

To describe how the presence of molecular bridges leads to longer G_0 plateaus in $G(Z)$ -curves, we present a tentative model, which is depicted in the inset of Figure 3. Here, we have translated scenario II into a simple spring model [8, 25, 26]. The atomic contact itself will generally be a gold dimer [8, 27]. The role of the n molecular bridges is to form n parallel springs, strengthening the junction. The attachment of the dimer to the first atomic layers of each of the electrodes can be described by a spring k_1 [8]. The elastic properties of the remainder of the electrode (the bulk of the electrode) can also be described by a spring k_2 . This description is similar to that of Torres *et al.*, where the contact is modeled as a series of N slices with a spring, k_n [25]. As for the molecular bridges, we assume that they are rigid, i.e. all displacements take place in between gold atoms [28]. We note that the Au-S bond is stronger than the Au-Au bond itself [29]. Hence, the weakest link of the molecular bridge is formed by the very gold atom that binds to the molecular S atom. This gold atom is itself attached to the first atomic layers of the electrode by a spring, with spring constant $k \approx k_1$, which is again attached to the remainder of the electrode. In total, we have $n + 1$ identical springs (1 due to the dimer, n due to the dithiols), which are in turn attached to the bulk electrode spring k_2 . The total spring constant equals $k_{tot} = \frac{a(n+1)}{a(n+1)+1}k_2$, where $a = k_1/k_2$. To break the dimer, the two gold atoms should be pulled apart by a force $F_0 \approx 1.5\text{nN}$ [30]. In the absence of dithiol molecules, this happens after the pushing rod has traveled a critical distance Z_0 . However, in the presence of n parallel springs, a greater total force F_n is to be applied over the junction, i.e., $F_n = F_0(n + 1)$. This force is also felt by springs k_2 , which are consequently elongated extra. Hence, the pushing rod has to be pushed further, over a distance Z_n to finally break the dimer. Our simple model yields $\frac{Z_n}{Z_0} = \frac{a(n+1)+1}{a+1}$.

From the experiment (see Table 1), we find that the increase in plateau length with respect to pure toluene is consistently more pronounced for BDT and ODT data sets with $\frac{Z_n}{Z_0} \approx 2\text{-}3$. Olesen *et al.* have shown that when making contact with a metal STM tip to a metal surface, approximately 1/4 of the initial displacement takes place between the last atom of the tip and the first layer of the surface metal atoms [26]. The other 3/4 takes place in the neighboring metal layers. Applying these numbers, such that $a \approx 3$, we get a consistent picture in which a few (typically 1 to 3) molecules bridge the atomic junction before it breaks ($\frac{Z_1}{Z_0} = 7/4$, $\frac{Z_2}{Z_0} = 10/4$ and $\frac{Z_3}{Z_0} = 13/4$).

After the atomic junction breaks, the metal-molecule-metal bridges become observable in the conductance, as seen for ODT. Remarkably, the stabilization effect in the contact regime is also observed for BDT (Figure 3), while no peak in the out-of-contact regime appears (Figure 2). This indicates that BDT bridges break during JOC. Most likely, this is due to an 'avalanche' effect: a sudden strain relief at JOC disrupts all junctions present. Short molecular bridges, such as gold-BDT-gold, are likely to bridge both electrodes in a stretched conformation, without so-called gauche defects. Such a conformation is rigid and is unlikely to accommodate a sudden distance jump of a few Å. Long molecular bridges, such as gold-ODT-gold, are less rigid, especially when they are in a bent conformation due to gauche defects [5, 10]. Therefore, they are less likely to be disrupted by JOC and explain why ODT does show plateaus in the out-of-contact regime.

We are not aware of any conductance measurements using forced gold-gold contact which show formation of metal-molecule-metal bridges of alkanedithiols smaller than 1,6-hexanedithiol [9]. However, a slightly alternative approach was reported by Li *et al.* and Haiss *et al.* [10, 11, 32, 33]. Here, gold-gold contact was avoided and electrodes with relatively low alkanedithiol coverage were used. In this way, alkanedithiol junctions as small as 1,5-pentanedithiol were measured and a strong preference for single molecule junctions was observed. Li *et al.* could even distinguish different conformations and couplings of a *single* molecular bridge. Our simple spring model helps to qualitatively understand the differences in data quality found in literature. In the experiments of Li *et al.* and Haiss *et al.* no gold bridge is present. Therefore, molecular junctions are not disrupted by the strain release during JOC, such that clear signals of (short) alkanedithiol bridges are observed.

In summary, we discuss new aspects of molecular bridge formation in break junction experiments in solutions of dithiolated molecules. We find that, in order to break a single atom contact, the electrodes have to be displaced 2-3 times longer in the presence of alkanedithiols as compared to the displacement when only solvent is present. This observation provides evidence for a scenario in which a few molecules already span the atomically thin gold neck before breaking, thereby reinforcing the atomic contact. Although present before JOC, metal-molecule-metal bridges only become 'observable' in the conductance when the metal bridge breaks. Our data are supported by a simple spring model. We put forward an important notion: A molecular bridge should be able to accommodate the strain release upon JOC in order to form a stable metal-molecule-metal bridge. For alkanedithiols at room temperature we find that the cross-over is between butanedithiol and octanedithiol.

Acknowledgements The authors acknowledge Bernard Wolfs and Siemon Bakker for technical support, Maarten Smid for his assistance in calibrating the setup and Oetze Staal for supplying purified toluene. This work was financed by the Netherlands Organisation for Scientific Research, NWO, and by the Zernike Institute for Advanced Materials.

References

- [1] Katsonis, N.; Kudernac, T.; Walko, M.; van der Molen, S.J.; van Wees, B.J.; Feringa, B.L. *Adv. Mat.* **2006**, 18, 1397-1400.
- [2] Lörtscher, E.; Ciszek, J.W.; Tour, J.; Riel, H. *Small* **2006**, 2, 973-977.
- [3] Elbing, M.; Ochs, R.; Koentopp, M.; Fischer, M.; Von Hänisch, K.; Weigend, F.; Evers, F.; Weber, H.B.; Mayor, M. *Proc. Natl. Acad. Sci.* **2005**, 102, 8815-8820.
- [4] Chen, F.; Hihath, J.; Huang, Z.; Li, X.; Tao, N.J. *Annu. Rev. Phys. Chem.* **2007**, 58, 535-564.
- [5] Akkerman, H.B.; de Boer, B. *J. Phys.: Condens. Matter* **2008**, 20, 013001.
- [6] Xu, B.; Tao, N. *Science* **2003**, 301, 1221-1223.
- [7] See for a review: Agrait, N.; Yeyati, A.L.; van Ruitenbeek, J.M. *Physics Reports* **2003**, 377, 81-279 and references therein.
- [8] Trouwborst, M.L.; Huisman, E.H.; Bakker, F.L.; van der Molen, S.J.; van Wees, B.J. *Phys. Rev. Lett.* **2008**, 100, 175502.
- [9] Li, X.; He, J.; Hihath, J.; Xu, B.; Lindsay, S.M.; Tao, N.J. *J. Am., Chem., Soc.* **2006**, 128, 2135-2141.
- [10] Li, C.; Pobelov, I.; Wandlowski, Th.; Bagrets, A.; Arnold, A.; Evers, F. *J. Am. Chem. Soc.* **2008**, 130, 318-326.
- [11] Haiss, W.; Nichols, R.J.; Van Zalinge, H.; Higgins, S. J.; Bethell, D.; Schriffin, D.J. *Phys. Chem. Chem. Phys* **2004**, 6, 4330-4337.
- [12] Venkataraman, L.; Klare, J.E.; Tam, I.W.; Nuckolls, C.; Hybertsen, M.S.; Steigerwald, M.L. *Nano Lett.*, **2006**, 6, 458-462.

- [13] Gonzàlez, M.T.; Wu, S.; Huber, R.; van der Molen, S.J.; Schönenberger, C.; Calame, M. *Nano Lett.*, **2006**, 6, 2238-2242.
- [14] Tsutsui, M.; Shoji, K.; Morimoto, K.; Taniguchi, M.; Kawai, T. *Appl. Phys. Lett.*, **2008**, 92, 223110 (3 pp).
- [15] Venkataraman, L.; Klare, J.E.; Nuckolls, C.; Hybertsen, M.S.; Steigerwald, M.L. *Nature*, **2006**, 442, 904-907.
- [16] Xu, B.; Zhang, P.; Li, X.; Tao, N. *Nano Lett.*, **2004**, 6, 1105-1108.
- [17] Suzuki, M., Fuji, S.; Fujihara, M. *Jap. J. Appl. Phys.* **2006**, 45, 2041-2044.
- [18] Martin, C.A.; Ding, D.; Van der Zant, H.S.J.; van Ruitenbeek, J.M. *New J. Phys* **2008**, 10, 065008.
- [19] Hihath, J.; Arroyo, C. R.; Rubio-Bollinger, G.; Tao, N.J. Agraït, N. *Nano Lett.* **2008**, 8 , 1673-1678.
- [20] For a detailed description of the setup used here, see supplementary information. Also see: Grüter, L.; Gonzàlez, M.T.; Huber, R.; Calame, M.; Schönenberger, C. *Small* **2005**, 1, 1067-1070.
- [21] Vrouwe, S.A.G.; van der Giessen, E.; van der Molen, S.J.; Dulic, D.; Trouwborst, M. L.; van Wees, B.J. *Phys. Rev. B.* **2005**, 71, 35313-35319.
- [22] van Houten, H.; Beenakker, C. *Physics Today* **1996**, July, 22-29.
- [23] Tsutsui, M.; Shoji, K.; Taniguchi, M.; Kawai, T. *Nano Lett.*, **2008**, 8, 345-349.
- [24] Yanson, A.I.; Rubio Bollinger, G.; van den Brom, H.E.; Agraït, N.; van Ruitenbeek, J.M. *Nature* **1998**, 395, 783-785.
- [25] Torres, J.A. and Sáenze, J.J. *Phys. Rev. Lett.* **1996**, 77, 2245-2248.
- [26] Olesen, L.; Brandbyge, M.; Sorensen, M.R.; Jacobsen, K.W.; Laegsgaard, E.; Stensgaard, I.; Besenbacher, F. *Phys. Rev. Lett.* **1996**, 76, 1485-1488.
- [27] Untiedt, C.; Caturla, M.J.; Calvo, M.R.; Palacios, J.J.; Segers, R. C.; van Ruitenbeek, J.M. *Phys. Rev. Lett.* **2007**, 98, 206801.
- [28] Huang, Z.; Chen, F.; Benett, P.A.; Tao, N.J. *J. Am. Chem. Soc.* **2007**, 129, 13225-13231.

- [29] Xu, B.; Xiao, X.; Tao, N.J. *J. Am. Chem. Soc.* **2003**, 125, 16164-16165.
- [30] Rubio-Bollinger, G.; Bahn, S.R.; Agraït, N.; Jacobsen, K.W.; Vieira, S. *Phys. Rev. Lett.* **2001**, 87, 026101.
- [31] Xia, J.L.; Diez-Perez, I.; Tao, N.J., *Nano Lett.* **2008**, on-line, DOI: 10.1021/nl080857a.
- [32] Mészáros, G.; Li, C.; Pobelov, I.; Wandlowski, T. *Nanotechnology* **2007**, 18, 424004.
- [33] Haiss, W.; van Zalinge, H.; Bethell, D.; Ulstrup, J.; Schriffin, D.J.; Nichols, R.J. *Faraday Discuss.* **2006**, 131, 253-264.
- [34] Costa-Krämer, J.L. *Phys. Rev. B.* **1997**, 55, R4875-R4878.

Sample	TOL1	TOL2	TOL3	BDT1	BDT2	ODT1	ODT2
Number of traces	250	250	150	300	50	300	150
Mean plateau length (μm)	0.62	0.74	0.65	2.02	2.01	1.55	1.58

Table 1: Table summarizing the number of traces and the mean plateau length of 7 different samples. The plateau length for each trace is defined as the length (in units of Z) of the plateau between 0.5 and 1.5 G_0 . The mean plateau length was determined by dividing the sum of all plateau lengths by the number of traces.

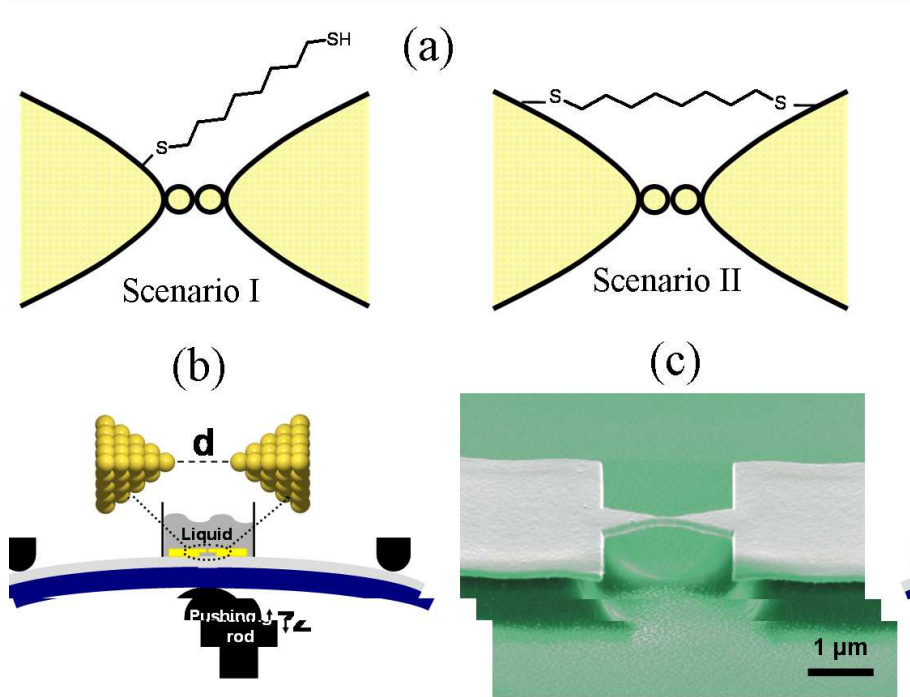


Figure 1: **(a)** Two possibilities for the position of a dithiolated molecule just before breaking of the gold wire. In I, the molecule is attached to one side of the electrode only. In II, the molecule is attached to both electrodes. **(b)** Schematic drawing of the MCBJ technique showing the liquid cell on top of the microfabricated gold leads on the flexible substrate clamped in a three-point bending configuration. **(c)** Scanning electron micrograph showing the suspended gold bridge on top of the polyimide layer.

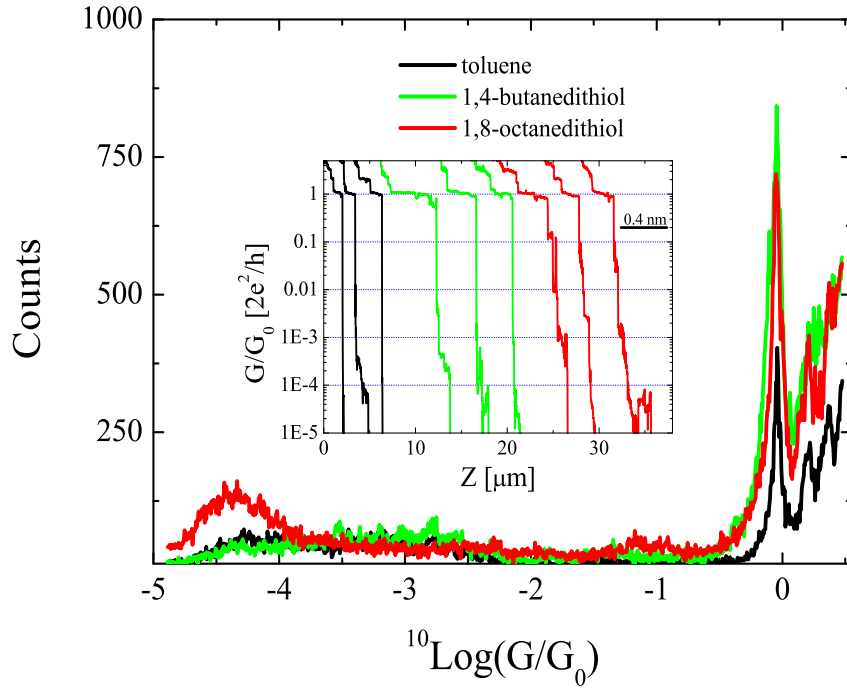


Figure 2: Logarithmic conductance histogram of 250 opening traces in toluene of sample TOL1 (black), in 10 mM BDT of sample BDT1 (green) and in 10 mM ODT of sample ODT1 (red). The conductances values were collected in bins of $0.0054 \cdot 10 \text{Log}(G/G_0)$. The inset displays 3 sample traces for each solution. The scale bar shows the actual electrode displacement d . The data has been corrected for an effective series resistance of $490 \, \Omega$ [34].

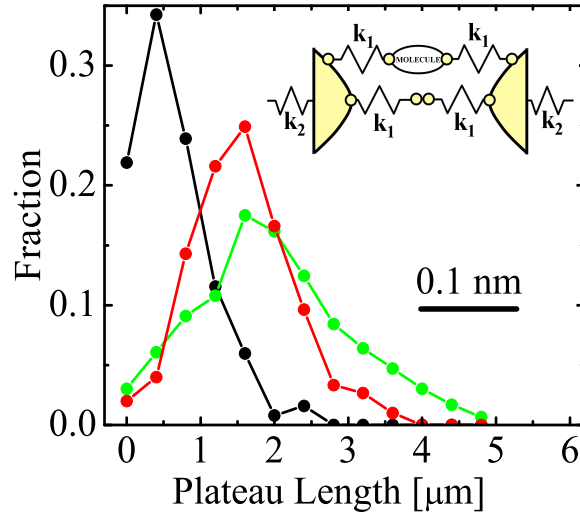


Figure 3: Plateau length histogram of 250 opening traces in toluene of sample TOL1 (black), 300 opening traces in 10 mM BDT of sample BDT1 (green) and 300 opening traces in 10 mM ODT of sample ODT1 (red). The bins are linear in units of Z . The plateau length is defined as the length (in units of Z) of the plateau between 0.5 and $1.5 G_0$. The inset shows a simple spring model to explain the increase in G_0 plateau length. The model incorporates alkane dithiols as parallel bridges in accordance with scenario II in Figure 1(a).